Available online at http://scik.org
Commun. Math. Biol. Neurosci. 2025, 2025:97
https://doi.org/10.28919/cmbn/9287
ISSN: 2052-2541

MODELING AND ANALYSIS OF AN *SIQRC* SYSTEM WITH FRACTIONAL DIFFERENTIAL EQUATIONS, CROSS-IMMUNITY, AND INHIBITORY EFFECTS

DEEPIKA SOLANKI[1], SUMIT KAUR BHATIA[1,*], STEVE MARTIN ANTHONY[1], PRAVEEN KUMAR[2]

[1]Department of Mathematics, Amity Institute of Applied Sciences, Amity University Uttar Pradesh, Noida 201301, India

[2]Department of Mathematics, Ramjas College, University of Delhi 110007, India

Abstract. This paper presents an *SIQRC* epidemic model formulated using fractional differential equations, incorporating a logistic growth rate and accounting for cross-immunity effects. The model further integrates inhibitory factors to assess their impact on disease transmission. We establish the non-negativity and boundedness of solutions, ensuring the biological feasibility of the model. We calculated the basic reproduction number, and the stability of equilibrium points is also analysed. Numerical simulations support the analytical findings highlighting the influence of the fractional order α on disease prevalance. Further, we investigate the influence of various parameters and inhibitory effects on disease prevalence. Additionally, we used Partial rank correlation coefficients and Latin hypercube sampling for global sensitivity analysis to determine key parameters affecting disease dynamics. This study provides valuable insights into the control and mitigation strategies for multi-strain infectious diseases.

Keywords: fractional differential equations; equilibrium points; local stability; global stability; global sensitivity analysis.

2020 AMS Subject Classification: 92B05, 92D25, 92D30.

*Corresponding author

E-mail address: sumit2212@gmail.com

Received April 12, 2025

1. INTRODUCTION

Infectious diseases have long been a threat to public health, with outbreaks causing widespread societal disruption and economic loss. From historical pandemics such as the Spanish Flu, which is estimated to have infected 500 million people globally, to recent outbreaks like COVID-19, which has caused over 777 million cases and nearly 7 million deaths worldwide by January 2024[1, 2], the rapid transmission of infectious diseases has repeatedly overwhelmed healthcare systems and destabilized economies. Understanding and controlling the spread of such diseases is crucial, and one powerful tool that has emerged in this context is mathematical modeling. By capturing the key mechanisms of disease transmission and progression, mathematical models offer valuable insights that help policymakers devise effective intervention strategies. Among the earliest and most influential models was the *SIR* model, introduced by Kermack and McKendrick in 1927[3]. This foundational model divided the population into three compartments - susceptible, infectious, and recovered - to describe the dynamics of disease outbreaks. Since the advent of the *SIR* model, researchers have made significant contributions to address the complexities of real-world disease transmission[4, 5, 6, 7, 8]. Subsequent models introduced additional compartments to capture different stages of infection, such as exposed individuals, asymptomatic, symptomatic, vaccinated, and quarantined populations[9, 5, 10, 11, 12]. However, a persistent limitation of these models is their reliance on ordinary differential equations, which does not take into account the memory effect of the disease. Unlike ODEs, fractional differential equations account for the fact that disease transmission and recovery processes can be influenced by their history, making them more reflective of real-world dynamics. Studies have shown that FDEs provide a more flexible and accurate framework for modeling disease over integer order[13, 14, 15, 16, 17, 18, 19]. For example, in [14], fractional order models have been shown to provide better predictions of plasma virus load than their integer-order counterparts. Similarly, in [18], based on the analysis of COVID-19 data from India and Brazil, it is observed that fractional-order derivative is more effective than integer order derivative.

Despite the progress made in modeling disease dynamics, several important aspects of multi-strain diseases remain underexplored. Multi-strain diseases such as influenza and COVID-19 exhibit complex transmission patterns, as individuals who recover from one strain may develop

partial immunity to others. This phenomenon, known as cross-immunity, can significantly alter the course of an outbreak due to subsequent strains. However, while several studies have introduced cross-immunity class in their models[9, 10, 20], there is a notable lack of research exploring these models through the lens of fractional order differential equations. Furthermore, limited attention has been given to the role of inhibitory factors such as individual behavior changes, which may significantly influence disease progression and control. In this paper, we extend the work of Paul et al. [18] , which focused on the dynamics of an *SIQR* epidemic model with a fractional order derivative. We introduce a *SIQRC* model which incorporates several key features that distinguish it from previous approaches. First, we model population growth using a logistic growth rate, which reflects the saturation effect as populations approach their carrying capacity. This is a more realistic assumption than the constant growth used in [18], as it accounts for the finite size of real-world populations and the limited resources available during an outbreak. Second, we include a cross-immune (C) class, representing individuals who have recovered from one strain of a disease and developed partial immunity to subsequent strains. This compartment allows us to explore the dynamics of multi-strain diseases more accurately, as cross-immunity affects both the speed and severity of future outbreaks. Additionally, we introduce inhibitory factors, which capture the effects of behavioral changes on the disease dynamics. These factors reflect the reality that disease transmission is not only a biological process but also a social one, influenced by individual and collective actions taken in response to an outbreak. The use of fractional differential equations (FDEs) in our model along with logistic growth rate, cross-immunity and inhibitory effects are the key aspects of its novelty. FDEs enhance the model's reliability by incorporating memory effects, which gives better prediction of disease spread. Moreover, the fractional approach allows us to explore the long-term effects of partial immunity, quarantine measures, and inhibitory factors in a way that traditional ODE models cannot.

The paper is divided into six sections. In Section 2, we outline the necessary preliminaries, including fundamental definitions and lemmas relevant to our analysis. Section 3 presents the formulation of the proposed *SIQRC* model. A comprehensive qualitative analysis of the model is conducted in Section 4, where we examine key properties such as non-negativity and

boundedness of solutions as well as local and global stability conditions for the equilibrium points. Section 5 summarizes the numerical results and global sensitivity analysis. Finally, Section 6 discusses key findings and potential directions for future research.

2. PRELIMINARIES

The various definitions related to fractional order differential equations are mentioned below:

Definition 1. [21] *The Caputo fractional derivative of order α, for a function $h(y) \in C^n([0,\infty),\mathbf{R})$ is defined as:*

$$^{C}D^{\alpha}(h(y)) = \frac{1}{\Gamma(n-\alpha)}\int_0^y \frac{h^n(\tau)}{(t-\tau)^{\alpha-n+1}}d\tau, \tag{1}$$

where $\tau \geq 0$, and n is a positive integer such that $n-1 \leq \alpha < n$, $\Gamma()$ describes the Gamma function.

Lemma 2. [21] *(Generalised Mean Value Theorem:) Let us assume that $h(y) \in C[c,d]$ and $^{C}D^{\alpha}h(y) \in C(c,d]$, for $0 < \alpha \leq 1$, then we have*

$$h(y) = h(c) + \frac{1}{\Gamma(\alpha)}(^{C}D^{\alpha}h)(\xi).(x-c)^{\alpha}$$

with $c \leq \xi \leq y$, $\forall\, y \in (c,d]$.

Lemma 3. [22] *Suppose that $h(t) \in C[c,d]$ and $^{C}D^{\alpha}h(t) \in C[c,d]$ for $0 < \alpha \leq 1$. If $^{C}D^{\alpha}h(t) \geq 0\ \forall\, t \in [c,d]$, then $h(t)$ is increasing for each $t \in [c,d]$. If $^{C}D^{\alpha}h(t) \leq 0\ \forall\, t \in [c,d]$, then $h(t)$ is decreasing for each $t \in [c,d]$.*

Definition 4. [19, 23] *For a given system using Caputo fractional derivative given by*

$$^{C}D^{\alpha}y(t) = u(t,y(t));\ y(0) = y_0;\ \alpha \in (0,1),$$

A point y^* is called an equilibrium point of the system if it satisfies $u(t,y^*) = 0$ and it is locally asymptotically stable if all eigenvalues λ_j of the Jacobian matrix J evaluated at this point satisfy $|arg(\lambda_j)| > \frac{\alpha\pi}{2}$.

Lemma 5. *(Boundedness)* [24] *Let $\alpha_1 > 0$, $\alpha_2 > 0$ and $c \in C$. Define*

$$y(t) = t^{\alpha_2 - 1} E_{\alpha_1,\alpha_2}(\pm c t^{\alpha_1}),$$

where $E_{\alpha_1,\alpha_2}(z)$ denotes the two parameter Mittag-Leffler function with parameters α_1 and α_2. Then the Laplace transformation of $y(t)$ is given by

$$\mathscr{L}[y(t)] = \frac{s^{\alpha_1 - \alpha_2}}{s^{\alpha_1} \mp c}.$$

Lemma 6. [24] *Let α_2 is an arbitrary real number. If $\alpha_1 < 2$, then there is a constant D_E such that, for all z in the complex plane,*

$$|E_{\alpha_1,\alpha_2}(z)| \leq \frac{D_E}{1 + |z|}.$$

Lemma 7. [17] *For a given characteristic equation:*

$$C(\eta) = \eta^n + a_1 \eta^{n-1} + a_2 \eta^{n-2} + ... + a_n = 0. \tag{2}$$

The condition (3) is satisfied by all of the roots of the characteristic equation (2) under the following conditions (1-5):

$$|arg(Eig(J^*))| = |arg\lambda_j| > \frac{\alpha\pi}{2} for all\, j = 1,2,3,4. \tag{3}$$

(1) For $n = 1$, the condition for (3) is $a_1 > 0$.

(2) For $n = 2$, the conditions for (3) are either Routh-Hurwitz conditions or $a_1 < 0$, $4a_2 > a_1^2$, $\left| tan^{-1}\left(\frac{\sqrt{4a_2 - (a_1)^2}}{a_1}\right)\right| > \frac{\alpha\pi}{2}$.

(3) For n=3, if the discriminant of $C(\eta)$ is positive, the necessary and sufficient conditions for (3) are $a_1 > 0$, $a_3 > 0$, $a_1 a_2 > a_3$, if $|C(\eta)| > 0$.

(4) If $|C(\eta)| < 0$, $a_1 > 0$, $a_2 > 0$, $a_1 a_2 = a_3$ then condition (3) is satisfied for all $\alpha \in [0,1)$.

(5) For general n, $a_n > 0$ is necessary for condition (3).

3. Mathematical Model Formulation

The formulation of the *SIQRC* model is discussed in this section, which is a compartmental epidemiological model that can be used to analyze the progression of an infectious disease. The model divides the population into five compartments: susceptible (P_s), infected (P_i), quarantined (P_q), recovered (P_r), and cross-immune (P_c). To establish a foundational framework, we first

present the *SIQRC* model in its classical integer-order form. The population of susceptible individuals grows with a logistic growth rate represented by the term $\tilde{r}P_s(t)\left(1-\frac{P_s(t)}{k}\right)$, where $\tilde{r}$ and k represent intrinsic growth rate and carrying capacity of susceptible population, respectively, while $P_s(t)$ decreases due to the contact of susceptibles and infected individuals, leading to disease transmission represented by the term $\frac{\tilde{\beta}P_s(t)P_i(t)}{1+\tilde{\alpha_1}P_s(t)+\tilde{\alpha_2}P_i(t)}$, where $\tilde{\beta}$ is the rate of transmission of disease and $\tilde{\alpha_1}$, $\tilde{\alpha_2}$ are the measure of inhibition effects such as preventive measures taken by susceptible individuals and crowding effect[10]. The growth in the number of susceptibles also occurs when cross-immune individuals lose partial immunity to disease and become susceptible again at a rate of $\tilde{\beta_1}$. $P_i(t)$ increases with the contact of susceptible and infected individuals, leading to disease transmission represented by the term $\frac{\tilde{\beta}P_s(t)P_i(t)}{1+\tilde{\alpha_1}P_s(t)+\tilde{\alpha_2}P_i(t)}$, where the parameters $\tilde{\beta},\tilde{\alpha_1},\tilde{\alpha_2}$ are as discussed above. $P_i(t)$ also grows due to the reinfection in cross-immune individuals represented by the term $\sigma\tilde{\xi}P_c(t)P_i(t)$ and decreases due to the quarantine of individuals at a rate of $\tilde{\gamma}$, disease-induced death at the rate of $\tilde{\mu_1}$ and natural death at rate of $\tilde{\mu}$. The quarantined class grows when $P_i(t)$ are quarantined at a rate of $\tilde{\gamma}$ and decreases with the recovery of these individuals at a rate of $\tilde{\delta}$, disease-induced death at the rate of $\tilde{\mu_1}$ and natural death rate $\tilde{\mu}$. The recovered population grows with the recovery of quarantined individuals while it decreases as individuals become cross-immune at a rate of γ_1 or experience natural mortality at the rate of $\tilde{\mu}$. The cross-immune population grows when recovered individuals lose total immunity and develop partial immunity to the disease at the rate $\tilde{\gamma_1}$, and decreases as individuals become susceptible again or face natural death at the rates $\tilde{\beta_1}$ and $\tilde{\mu}$, respectively. Hence,

$$
\left.\begin{aligned}
\frac{dP_s}{dt} &= \tilde{r}P_s(t)\left(1-\frac{P_s(t)}{k}\right)-\frac{\tilde{\beta}P_s(t)P_i(t)}{1+\tilde{\alpha_1}P_s(t)+\tilde{\alpha_2}P_i(t)}+\tilde{\beta_1}P_c(t),\\
\frac{dP_i}{dt} &= \frac{\tilde{\beta}P_s(t)P_i(t)}{1+\tilde{\alpha_1}P_s(t)+\tilde{\alpha_2}P_i(t)}-(\tilde{\gamma}+\tilde{\mu}+\tilde{\mu_1})P_i(t)+\sigma\tilde{\xi}P_c(t)P_i(t),\\
\frac{dP_q}{dt} &= \tilde{\gamma}P_i(t)-(\tilde{\delta}+\tilde{\mu}+\tilde{\mu_1})P_q(t),\\
\frac{dP_r}{dt} &= \tilde{\delta}P_q(t)-\tilde{\mu}P_r(t)-\tilde{\gamma_1}P_r(t)+(1-\sigma)\tilde{\xi}P_c(t)P_i(t),\\
\frac{dP_c}{dt} &= \tilde{\gamma_1}P_r(t)-\tilde{\xi}P_c(t)P_i(t)-\tilde{\mu}P_c(t)-\tilde{\beta_1}P_c(t).
\end{aligned}\right\} \tag{4}
$$

To enhance the model's realism, we incorporate the Caputo fractional derivative to the above system, which accounts for the system's past states and provides a more generalized representation of disease dynamics. The modified model is as under:

$$
\left.
\begin{aligned}
{}^{C}D^{\alpha}P_s(t) &= \tilde{r}^{\alpha}P_s(t)\left(1-\frac{P_s(t)}{k}\right)-\frac{\tilde{\beta}^{\alpha}P_s(t)P_i(t)}{1+\tilde{\alpha_1}P_s(t)+\tilde{\alpha_2}P_i(t)}+\tilde{\beta_1}^{\alpha}P_c(t),\\
{}^{C}D^{\alpha}P_i(t) &= \frac{\tilde{\beta}^{\alpha}P_s(t)P_i(t)}{1+\tilde{\alpha_1}P_s(t)+\tilde{\alpha_2}P_i(t)}-(\tilde{\gamma}^{\alpha}+\tilde{\mu}^{\alpha}+\tilde{\mu_1}^{\alpha})P_i(t)+\sigma\tilde{\xi}^{\alpha}P_c(t)P_i(t),\\
{}^{C}D^{\alpha}P_q(t) &= \tilde{\gamma}^{\alpha}P_i(t)-(\tilde{\delta}^{\alpha}+\tilde{\mu}^{\alpha}+\tilde{\mu_1}^{\alpha})P_q(t),\\
{}^{C}D^{\alpha}P_r(t) &= \tilde{\delta}^{\alpha}P_q(t)-\tilde{\mu}^{\alpha}P_r(t)-\tilde{\gamma_1}^{\alpha}P_r(t)+(1-\sigma)\tilde{\xi}^{\alpha}P_c(t)P_i(t),\\
{}^{C}D^{\alpha}P_c(t) &= \tilde{\gamma_1}^{\alpha}P_r(t)-\tilde{\xi}^{\alpha}P_c(t)P_i(t)-\tilde{\mu}^{\alpha}P_c(t)-\tilde{\beta_1}^{\alpha}P_c(t).
\end{aligned}
\right\} \tag{5}
$$

For simplicity, let $\tilde{r}^{\alpha}=r,\ \tilde{\beta}^{\alpha}=\beta,\ \tilde{\alpha_1}=\alpha_1,\ \tilde{\alpha_2}=\alpha_2, \tilde{\beta_1}^{\alpha}=\beta_1,\ \tilde{\gamma}^{\alpha}=\gamma,\ \tilde{\mu}^{\alpha}=\mu,\ \tilde{\mu_1}^{\alpha}=\mu_1,\ ,\ \tilde{\xi}^{\alpha}=\xi,\ \tilde{\delta}^{\alpha}=\delta,\ \tilde{\gamma_1}^{\alpha}=\gamma_1$.

Thus, on the basis of the aforementioned assumptions, the system is as follows:

$$
\left.
\begin{aligned}
{}^{C}D^{\alpha}P_s(t) &= rP_s(t)\left(1-\frac{P_s(t)}{k}\right)-\frac{\beta P_s(t)P_i(t)}{1+\alpha_1P_s(t)+\alpha_2P_i(t)}+\beta_1P_c(t),\\
{}^{C}D^{\alpha}P_i(t) &= \frac{\beta P_s(t)P_i(t)}{1+\alpha_1P_s(t)+\alpha_2P_i(t)}-(\gamma+\mu+\mu_1)P_i(t)+\sigma\xi P_c(t)P_i(t),\\
{}^{C}D^{\alpha}P_q(t) &= \gamma P_i(t)-(\delta+\mu+\mu_1)P_q(t),\\
{}^{C}D^{\alpha}P_r(t) &= \delta P_q(t)-\mu P_r(t)-\gamma_1P_r(t)+(1-\sigma)\xi P_c(t)P_i(t),\\
{}^{C}D^{\alpha}P_c(t) &= \gamma_1P_r(t)-\xi P_c(t)P_i(t)-\mu P_c(t)-\beta_1P_c(t).
\end{aligned}
\right\} \tag{6}
$$

where the initial conditions for system (6) are:

$$P_s(0)>0, P_i(0)\geq 0, P_q(0)\geq 0, P_r(0)\geq 0, P_c(0)\geq 0. \tag{7}$$

To be biological meaningful, all parameters are assumed to be non-negative as given in Table 1.

Parameter	Relevant Biological Description
r	Intrinstic Growth Rate
k	Carrying Capacity
β	Rate of transmission from $P_s(t)$ to $P_i(t)$
α_1, α_2	Inhibitory Factors
β_1	Rate at which cross-immune population becomes susceptible again
γ	Rate at which infected are quarantined
μ	Natural Death Rate
μ_1	Disease-induced Death Rate
σ	Average reinfection probability of cross-immune individual
ξ	Transmission rate from $P_i(t)$ to $P_c(t)$
δ	Recovery rate
γ_1	Rate at which recovered population becomes cross-immune

TABLE 1. Parameters and their relevance

4. QUALITATIVE ANALYSIS OF MODEL (6)

In this section, we analyze the qualitative properties of the proposed *SIQRC* model to understand its long-term behavior. We begin by investigating the non-negativity and boundedness of the model's solution. Establishing positivity ensures that all state variables remain biologically meaningful, as negative population values are not feasible in real-world. Additionally, stability analysis is performed to determine the specific conditions under which the disease-free and endemic equilibria remain stable. The global stability of the endemic equilibrium point is also examined.

4.1. Positivity and boundedness of solutions of model (6).

Theorem 8. *The solution* $(P_s(t), P_i(t), P_q(t), P_r(t), P_c(t)) \in \mathbf{R}^5$ *of the model (6) remains non-negative under given initial conditions (7) for* $t \geq 0$. *Further,*

$\Omega = \left\{ \big(P_s(t), P_i(t), P_q(t), P_r(t), P_c(t)\big) \in \mathbf{R}^5_+ : P_N(t) \leq \dfrac{rk}{\hat{\mu}} \right\}$ *is a positively-invarient set for model (6).*

Proof. From model (6), we have,

${}^{C}D^{\alpha}P_s(t)|_{P_s(t)=0} = \beta_1 P_c(t) \geq 0$, ${}^{C}D^{\alpha}P_i(t)|_{P_i(t)=0} = 0$, ${}^{C}D^{\alpha}P_q(t)|_{P_q(t)=0} = \gamma P_i(t) \geq 0$, ${}^{C}D^{\alpha}P_r(t)|_{P_r(t)=0} = \delta P_q(t) + (1-\sigma)\xi P_c(t)P_i(t) \geq 0$, ${}^{C}D^{\alpha}P_c(t)|_{P_c(t)=0} = \gamma_1 P_r(t) \geq 0$.

As the aforementioned values are non-negative on the border planes, we will constantly stay inside the closed 5-dimensional space $\mathbb{R}^5_+$. This is due to the inward orientation of the vector field on all boundary planes. Therefore, using Lemma 2 and Lemma 3 it is established that all solutions of the model (6) are non-negative.

Hence let's assume, $P_N(t) = P_s(t) + P_i(t) + P_q(t) + P_r(t) + P_c(t)$. Then, we obtain

$$ {}^{C}D^{\alpha}P_N(t) \leq rk - \hat{\mu}P_N(t),\ \hat{\mu} = \min\{r, \mu\}$$

We define the initial value problem as follows:

$$ {}^{C}D^{\alpha}\overline{P_N} = rk - \hat{\mu}\overline{P_N}(t),\ \overline{P_N}(0) = \overline{P_{N_0}}, \tag{8}$$

Applying Laplace transform to equation (8), we derive

$$ s^{\alpha}\mathscr{L}(\overline{P_N}(t)) - s^{\alpha-1}\overline{P_{N_0}} = \frac{(rk)}{s} - \hat{\mu}\mathscr{L}(\overline{P_N(t)}),$$

$$ \implies \mathscr{L}(\overline{P_N(t)}) = \frac{s^{\alpha-1}\overline{P_{N_0}}}{s^{\alpha}+\hat{\mu}} + \frac{(rk)s^{-1}}{s^{\alpha}+\hat{\mu}}. \tag{9}$$

Using Lemma 5 and on taking inverse Laplace transform of equation (9), we get

$$ \overline{P_N(t)} = \overline{P_{N_0}}E_{\alpha,1}(-\hat{\mu}t^{\alpha}) + (rk)t^{\alpha}E_{\alpha,\alpha+1}(-\hat{\mu}t^{\alpha}). \tag{10}$$

Using Comparison principle [25], equation (10) and Lemma 6:

$$ P_N(t) \leq \frac{\overline{P_{N_0}}D_E}{1+\hat{\mu}t^{\alpha}} + \frac{(rk)t^{\alpha}D_E}{1+\hat{\mu}t^{\alpha}}.$$

Thus, $\limsup_{t\to\infty} P_N(t) = \dfrac{rk}{\hat{\mu}}$. Hence, $P_N(t) \leq \dfrac{rk}{\hat{\mu}}$ and therefore,

$$ \Omega = \left\{ \big(P_s(t), P_i(t), P_q(t), P_r(t), P_c(t)\big) \in \mathbb{R}^5_+ : P_N(t) \leq \frac{rk}{\hat{\mu}} \right\} \tag{11}$$

is positively invariant with respect to the system(6). □

4.2. Existence of Equilibrium Points. The equilibrium points are obtained by solving ${}^{C}D^{\alpha}P_s(t)=0$, ${}^{C}D^{\alpha}P_i(t)=0$, ${}^{C}D^{\alpha}P_q(t)=0$, ${}^{C}D^{\alpha}P_r(t)=0$ and ${}^{C}D^{\alpha}P_c(t)=0$. Therefore, we obtain the following equilibrium points:

(1) Disease-free equilibrium point ($D.F.E$):

$$\mathscr{P}_1=(P_s^0,P_i^0,P_q^0,P_r^0,P_c^0)=(k,0,0,0,0)\,.$$

(2) Endemic equilibrium point ($E.E.P$):

$$\mathscr{P}_2=(P_{s_1}^*,P_{i_1}^*,P_{q_1}^*,P_{r_1}^*,P_{c_1}^*),$$

From ${}^{C}D^{\alpha}P_q(t)=0$, we get

$$P_{q_1}^*=\frac{\gamma P_{i_1}^*}{\delta+\mu+\mu_1}.$$

Now, let ${}^{C}D^{\alpha}P_r(t)=0$ and substituting value of P_{q1}^* from above, we get:

$$P_{r_1}^*=\frac{\delta\gamma P_{i_1}^*}{(\mu+\gamma_1)(\delta+\mu+\mu_1)}+\frac{(1-\sigma)\xi P_{c_1}^* P_{i_1}^*}{\mu+\gamma_1}.$$

Next, let ${}^{C}D^{\alpha}P_c(t)=0$ and substituting value of $P_{r_1}^*$, we get:

$$P_{c_1}^*=\frac{\delta\gamma\gamma_1 P_{i_1}^*}{(\delta+\mu+\mu_1)\left((\mu+\gamma_1)(\mu+\beta_1+\xi P_{i_1}^*)-(1-\sigma)\gamma_1\xi P_{i_1}^*\right)}.$$

Further, let ${}^{C}D^{\alpha}P_i(t)=0$ and substituting values of $P_{r_1}^*$, we get:

$$P_{s_1}^*=\frac{(1+\alpha_2 P_{i_1}^*)(\gamma+\mu+\mu_1-\sigma\xi P_{c_1}^*)}{\beta-\alpha_1(\gamma+\mu+\mu_1-\sigma\xi P_{c_1}^*)}.$$

Finally putting values of $P_{s_1}^*$, $P_{q_1}^*$, $P_{r_1}^*$ and $P_{c_1}^*$ in ${}^{C}D^{\alpha}P_s(t)=0$ we obtain:

$$F_1P_{i_1}^{*6}+F_2P_{i_1}^{*5}+F_3P_{i_1}^{*4}+F_4P_{i_1}^{*3}+F_5P_{i_1}^{*2}+F_6P_{i_1}^{*}+F_7=0. \tag{12}$$

where values of $F_1,F_2,F_3,F_4,F_5,F_6,F_7$ are given in Appendix.

If one of the following conditions is true, then the positive solution of equation (12) will exist and thus endemic equilibrium point will exist. The conditions are as follows:

- $F_i<0,F_j>0\ \forall i=1;j=2,3,4,5,6,7.$
- $F_i<0,F_j>0\ \forall i=1,2;j=3,4,5,6,7.$

- $F_i < 0, F_j > 0 \; \forall i = 1,2,3; j = 4,5,6,7.$
- $F_i < 0, F_j > 0 \; \forall i = 1,2,3,4; j = 5,6,7.$
- $F_i < 0, F_j > 0 \; \forall i = 1,2,3,4,5; j = 6,7.$
- $F_i < 0, F_j > 0 \; \forall i = 1,2,3,4,5,6; j = 7.$
- $F_i > 0, F_j < 0 \; \forall i = 1; j = 2,3,4,5,6,7.$
- $F_i > 0, F_j < 0 \; \forall i = 1,2; j = 3,4,5,6,7.$
- $F_i > 0, F_j < 0 \; \forall i = 1,2,3; j = 4,5,6,7.$
- $F_i > 0, F_j < 0 \; \forall i = 1,2,3,4; j = 5,6,7.$
- $F_i > 0, F_j < 0 \; \forall i = 1,2,3,4,5; j = 6,7.$
- $F_i > 0, F_j < 0 \; \forall i = 1,2,3,4,5,6; j = 7.$

Basic Reproduction Number, (R_0)***:*** The basic reproduction number R_0 is calculated using the next generation matrix approach[26]:

$$\mathscr{E} = \begin{bmatrix} \dfrac{\beta P_s P_i}{1+\alpha_1 P_s + \alpha_2 P_i} \\ 0 \end{bmatrix}, \; \mathscr{F} = \begin{bmatrix} (\gamma+\mu+\mu_1)P_i - \sigma\xi P_c P_i \\ -\gamma P_i + (\delta+\mu+\mu_1)P_q \end{bmatrix}$$

The Jacobian matrix for $\mathscr{E}$ and $\mathscr{F}$ obtained are:

$$\mathrm{E} = \begin{bmatrix} \dfrac{\beta P_s^0}{1+\alpha_1 P_s^0 + \alpha_2 P_i^0} - \dfrac{\beta\alpha_2 P_s^0 P_i^0}{(1+\alpha_1 P_s^0 + \alpha_2 P_i^0)^2} & 0 \\ 0 & 0 \end{bmatrix}$$

$$\text{and } \mathrm{F} = \begin{bmatrix} \gamma+\mu+\mu_1-\sigma\xi P_c^0 & 0 \\ -\gamma & (\delta+\mu+\mu_1) \end{bmatrix}$$

The next generation matrix is:

$$\mathscr{K} = EF^{-1} = \frac{1}{(\delta+\mu+\mu_1)(\gamma+\mu+\mu_1-\sigma\xi P_c^0)} \begin{bmatrix} \dfrac{\beta P_s^0(\delta+\mu+\mu_1)(1+\alpha_1 P_s^0)}{(1+\alpha_1 P_s^0+\alpha_2 P_i^0)^2} & 0 \\ 0 & 0 \end{bmatrix}.$$

Hence, the basic reproduction number is

$$R_0 = \frac{\beta k}{(\gamma+\mu+\mu_1)(1+\alpha_1 k)}. \tag{13}$$

4.3. Stability analysis of equilibrium points of the model (6).

4.3.1. *Local Stability analysis of D.F.E* $(\mathscr{P}_1)$*.* The linearised matrix at the Disease-free equilibrium point $\mathscr{P}_1$ is given as:

$$\mathscr{J}_1 = \begin{bmatrix} -r & -\frac{\beta k}{1+\alpha_1 k} & 0 & 0 & \beta_1 \\ 0 & \frac{\beta k}{1+\alpha_1 k} - \gamma - \mu - \mu_1 & 0 & 0 & 0 \\ 0 & \gamma & -(\delta+\mu+\mu_1) & 0 & 0 \\ 0 & 0 & \delta & -\mu-\gamma_1 & 0 \\ 0 & 0 & 0 & \gamma_1 & -\mu-\beta_1 \end{bmatrix}$$

The characteristics equation of the matrix $\mathscr{J}_1$ is as follows:

$$P_1(\lambda) = \lambda^5 + H_{11}\lambda^4 + H_{12}\lambda^3 + H_{13}\lambda^2 + H_{14}\lambda + H_{15} = 0. \tag{14}$$

where the coefficients H_{11}, H_{12}, H_{13} and H_{14} are given by:

$$\begin{aligned}
H_{11} &= (r+\beta_1+\delta+\gamma_1+\mu_1+3\mu) + \left(\gamma+\mu+\mu_1 - \frac{\beta k}{1+\alpha_1 k}\right), \\
H_{12} &= (\mu+\beta_1)\left(\delta+2\mu+\mu_1+\gamma_1+r+\left(\gamma+\mu+\mu_1-\frac{\beta k}{(1+\alpha_1 k)}\right)\right) + r(\mu+\gamma_1) \\
&\quad + \left(\gamma+\mu+\mu_1-\frac{\beta k}{1+\alpha_1 k}\right)(\delta+2\mu+\mu_1+\gamma_1+r) + (\delta+\mu+\mu_1)(\mu+\gamma_1+r), \\
H_{13} &= \left(\gamma+\mu+\mu_1-\frac{\beta k}{1+\alpha_1 k}\right)((\mu+\beta_1)(\delta+\mu+\mu_1) + (\mu+\beta_1)(\mu+\gamma_1) + r(\mu+\beta_1) \\
&\quad + (\mu+\gamma_1)(\delta+\mu+\mu_1) + r(\delta+\mu+\mu_1)) + (\delta+\mu+\mu_1)\,((\mu+\beta_1)(\mu+\gamma_1) \\
&\quad + r(\mu+\beta_1)) + (\mu+\gamma_1)\left(r(\mu+\beta_1) + r(\delta+\mu+\mu_1) + r\left(\gamma+\mu+\mu_1-\frac{\beta k}{1+\alpha_1 k}\right)\right), \\
H_{14} &= r(\mu+\gamma_1)(\mu+\beta_1)(\delta+\mu+\mu_1) + \left(\gamma+\mu+\mu_1-\frac{\beta k}{1+\alpha_1 k}\right) \\
&\quad (r(\mu+\gamma_1)(\mu+\beta_1) + r(\mu+\gamma_1)(\delta+\mu+\mu_1) + (\mu+\gamma_1)(\mu+\beta_1)(\delta+\mu+\mu_1) \\
&\quad r(\mu+\beta_1)(\delta+\mu+\mu_1), \\
H_{15} &= r(\mu+\gamma_1)(\mu+\beta_1)(\delta+\mu+\mu_1)\left(\gamma+\mu+\mu_1-\frac{\beta k}{(1+\alpha_1 k)}\right).
\end{aligned}$$

All the characteristic roots of equation (14) are given by $\lambda_1 = -r$, $\lambda_2 = -\mu-\gamma_1$, $\lambda_3 = -\delta-\mu-\mu_1$, $\lambda_4 = -\mu-\beta_1$, and $\lambda_5 = (\gamma+\mu+\mu_1)(R_0-1)$.

We see that the eigen values λ_1, λ_2, λ_3 and λ_4 of the characteristic equation are negative and the eigen value λ_5 will be negative if $R_0 < 1$. In addition to this, all coefficients of equation (14) satisfy condition (5) of Lemma 7. Hence,

$$|arg\lambda_j| = \pi > \frac{\alpha\pi}{2} \forall j = 1,2,3,4,5.$$

Now, if $R_0 > 1$, then eigenvalue $\lambda_5 > 0 \implies |arg\lambda_5| = 0 < \frac{\alpha\pi}{2}$ making the *D.F.E* $\mathscr{P}_1$ unstable. Therefore, using Matignon's condition[27, 23], we have the following theorem:

Theorem 9. *The D.F.E* $\mathscr{P}_1 = (k,0,0,0,0)$ *of the system (6) is locally asymptotically stable if the basic reproduction number* $R_0 < 1$ *and unstable when* $R_0 > 1$.

4.3.2. *Local Stability analysis of E.E.P (*$\mathscr{P}_2$*).* The linearised matrix of the model (6) at *E.E.P* $\mathscr{P}_2$ is obtained as:

$$\mathscr{J}_2 = \begin{bmatrix} a_0 & a_1 & 0 & 0 & a_2 \\ b_0 & b_1 & 0 & 0 & b_2 \\ 0 & c_0 & c_1 & 0 & 0 \\ 0 & d_0 & d_1 & d_2 & d_3 \\ 0 & e_0 & 0 & e_1 & e_2 \end{bmatrix}$$

where, $a_0 = r - \dfrac{2rP^*_{s_1}}{k} - \dfrac{\beta P^*_{i_1}(1+\alpha_2 P^*_{i_1})}{(1+\alpha_1 P^*_{s_1}+\alpha_2 P^*_{i_1})^2}$, $a_1 = -\dfrac{\beta P^*_{s_1}(1+\alpha_1 P^*_{s_1})}{(1+\alpha_1 P^*_{s_1}+\alpha_2 P^*_{i_1})^2}$,
$a_2 = \beta_1$, $b_0 = \dfrac{\beta P^*_{i_1}(1+\alpha_2 P^*_{i_1})}{(1+\alpha_1 P^*_{s_1}+\alpha_2 P^*_{i_1})^2}$, $b_1 = \dfrac{\beta P^*_{s_1}(1+\alpha_1 P^*_{s_1})}{(1+\alpha_1 P^*_{s_1}+\alpha_2 P^*_{i_1})^2} - \gamma - \mu - \mu_1 + \sigma\xi P^*_{c_1}$,
$b_2 = \sigma\xi P^*_{i_1}$, $c_0 = \gamma$, $c_1 = -\delta - \mu - \mu_1$, $d_0 = (1-\sigma)\xi P^*_{c_1}$, $d_1 = \delta$, $d_2 = -\mu - \gamma_1$,
$d_3 = (1-\sigma)\xi P^*_{i_1}$, $e_0 = -\xi P^*_{c_1}$, $e_1 = \gamma_1$, $e_2 = -\xi P^*_{i_1} - \mu - \beta_1$.

The characteristic equation of the above matrix is given by:

$$P_2(\lambda) = \lambda^5 + H_{21}\lambda^4 + H_{22}\lambda^3 + H_{23}\lambda^2 + H_{24}\lambda + H_{25} = 0. \tag{15}$$

where the coefficients $H_{21}, H_{22}, H_{23}, H_{24}$ and H_{25} are given by:

$$H_{21} = -(a_0 + b_1 + c_1 + d_2 + e_2),$$

$$H_{22} = -a_1b_0 + a_0b_1 + a_0c_1 + b_1c_1 + a_0d_2 + b_1d_2 + c_1d_2 - b_2e_0 - d_3e_1 + a_0e_2 + b_1e_2 + c_1e_2 + d_2e_2,$$

$$H_{23} = a_1b_0c_1 - a_0b_1c_1 + a_1b_0d_2 - a_0b_1d_2 - a_0c_1d_2 - b_1c_1d_2 - a_2b_0e_0 + a_0b_2e_0 + b_2c_1e_0 + b_2d_2e_0 - b_2d_0e_1 + a_0d_3e_1 + b_1d_3e_1 + c_1d_3e_1 + a_1b_0e_2 - a_0b_1e_2 - a_0c_1e_2 - b_1c_1e_2 - a_0d_2e_2 - b_1d_2e_2 - c_1d_2e_2,$$

$$H_{24} = -a_1b_0c_1d_2 + a_0b_1c_1d_2 + a_2b_0c_1e_0 - a_0b_2c_1e_0 + a_2b_0d_2e_0 - a_0b_2d_2e_0 - b_2c_1d_2e_0$$
$$- a_2b_0d_0e_1 + a_0b_2d_0e_1 + b_2c_1d_0e_1 - b_2c_0d_1e_1 + a_1b_0d_3e_1 - a_0b_1d_3e_1 - a_0c_1d_3e_1$$
$$- b_1c_1d_3e_1 - a_1b_0c_1e_2 + a_0b_1c_1e_2 - a_1b_0d_2e_2 + a_0b_1d_2e_2 + a_0c_1d_2e_2 + b_1c_1d_2e_2,$$
$$H_{25} = -a_2b_0c_1d_2e_0 + a_0b_2c_1d_2e_0 + a_2b_0c_1d_0e_1 - a_0b_2c_1d_0e_1 - a_2b_0c_0d_1e_1 + a_0b_2c_0d_1e_1$$
$$- a_1b_0c_1d_3e_1 + a_0b_1c_1d_3e_1 + a_1b_0c_1d_2e_2 - a_0b_1c_1d_2e_2.$$

If the above coefficients $H_{21}, H_{22}, H_{23}, H_{24}$ and H_{25} are positive for $\mathscr{P}_2$, then using condition (5) of Lemma 7, the $E.E.P$ $\mathscr{P}_2$ is locally asymptotically stable. Hence, we obtain the following theorem:

Theorem 10. *If the coefficients $H_{21}, H_{22}, H_{23}, H_{24}$ and H_{25} of equation (15) are positive, then $E.E.P$ $\mathscr{P}_2$ is locally asymptotically stable.*

4.3.3. *Global stability of $\mathscr{P}_2$.*

Theorem 11. *The $E.E.P$ $\mathscr{P}_2$ of the model(6) is globally asymptotically stable when the subsequent criteria's are met:*

(1) $\dfrac{rP^*_{s_1}}{k} > 3r + \beta_1 + \sigma\xi P^*_{c_1} + \gamma + \mu + \mu_1 + \dfrac{r^2}{\mu} + \dfrac{\sigma\xi rk}{\mu}$,

(2) $\mu + \mu_1 + \sigma\xi P^*_{c_1} > 3\sigma\xi P^*_{c_1} + r + 2\xi P^*_{c_1} + \beta_1 + \dfrac{rP^*_{s_1}}{k} + \dfrac{r^2}{\mu} + \dfrac{\sigma\xi rk}{\mu}$,

(3) $2\mu + \gamma_1 > \delta + (1-\sigma)\xi P^*_{c_1} + \dfrac{(1-\sigma)\xi rk}{\mu}$,

(4) $2\mu > +\gamma_1 + \xi P^*_{c_1} + \dfrac{\sigma\xi rk}{\mu}$,

(5) $\delta + 2\mu + 2\mu_1 > \gamma$.

Proof. Let us consider the function:

$$W(t) = \frac{1}{2}[(P_s - P^*_{s_1}) + (P_i - P^*_{i_1})]^2 + \frac{1}{2}(P_q - P^*_{q_1})^2 + \frac{1}{2}(P_r - P^*_{r_1})^2 + \frac{1}{2}(P_c - P^*_{c_1})^2 \tag{16}$$

On differentiation equation (16) along with the solutions of model (6), we get:

$$^{C}D^{\alpha}V(t)$$
$$= [(P_s - P^*_{s_1}) + (P_i - P^*_{i_1})]\left(rP_s(t)\left(1 - \frac{P_s(t)}{k}\right) + \beta_1 P_c(t) - (\gamma + \mu + \mu_1)P_i(t)\right.$$

$$+\sigma\xi P_c(t)P_i(t)) + (P_q - P^*_{q_1})\left(\gamma P_i(t) - (\delta+\mu+\mu_1)P_q(t)\right)$$

$$+ (P_r - P^*_{r_1})\left(\delta P_q(t) - \mu P_r(t) - \gamma_1 P_r(t) + (1-\sigma)\xi P_c(t)P_i(t)\right)$$

$$+ (P_c - P^*_{c_1})\left(\gamma_1 P_r(t) - \xi P_c(t)P_i(t) - \mu P_c(t) - \beta_1 P_c(t)\right),$$

$$\leq \left(\frac{3r}{2} - \frac{rP^*_{s_1}}{2k} + \frac{\beta_1}{2} + \frac{\sigma\xi rk}{2\mu} + \frac{\sigma\xi P^*_{c_1}}{2} + \frac{\gamma+\mu+\mu_1}{2} + \frac{r^2}{2\mu}\right)(P_s - P^*_{s_1})^2$$

$$\left(\frac{3\sigma\xi P^*_{c_1}}{2} - \frac{\mu}{2} - \frac{\mu_1}{2} + \frac{r}{2} + \frac{rP^*_{s_1}}{2k} + \frac{r^2}{2\mu} + \frac{\beta_1}{2} + \frac{\sigma\xi rk}{2\mu} + \xi P^*_{c_1} - \frac{\sigma\xi P^*_{c_1}}{2}\right)(P_i - P^*_{i_1})^2$$

$$\left(\frac{\delta}{2} - \mu - \frac{\gamma_1}{2} + \frac{(1-\sigma)\xi rk}{2\mu} + \frac{(1-\sigma\xi P^*_{c_1})}{2}\right)(P_r - P^*_{r_1})^2 + \left(\frac{\sigma\xi rk}{2\mu} + \frac{\gamma_1}{2} - \mu + \frac{\xi P^*_{c_1}}{2}\right)$$

$$(P_c - P^*_{c_1})^2 + \left(\frac{\gamma}{2} - \frac{\delta}{2} - \mu - \mu_1\right)(P_q - P^*_{q_1}).$$

Hence, ${}^C D^\alpha V(t) \leq 0$ when the inequalities given below holds true:

(1) $\dfrac{rP^*_{s_1}}{k} > 3r + \beta_1 + \sigma\xi P^*_{c_1} + \gamma + \mu + \mu_1 + \dfrac{r^2}{\mu} + \dfrac{\sigma\xi rk}{\mu}$,

(2) $\mu + \mu_1 + \sigma\xi P^*_{c_1} > 3\sigma\xi P^*_{c_1} + r + 2\xi P^*_{c_1} + \beta_1 + \dfrac{rP^*_{s_1}}{k} + \dfrac{r^2}{\mu} + \dfrac{\sigma\xi rk}{\mu}$,

(3) $2\mu + \gamma_1 > \delta + (1-\sigma)\xi P^*_{c_1} + \dfrac{(1-\sigma)\xi rk}{\mu}$,

(4) $2\mu > +\gamma_1 + \xi P^*_{c_1} + \dfrac{\sigma\xi rk}{\mu}$,

(5) $\delta + 2\mu + 2\mu_1 > \gamma$.

Thus according to LaSalle's invariance principle[28], the endemic equilibria of the model (6) is globally asymptomatically stable.

□

5. NUMERICAL SIMULATIONS

To perform the numerical simulations, the parameteric values have been taken as in Table 2 and the initial population sizes are taken as $P_s(0) = 1$, $P_i(0) = 1$, $P_q(0) = 1$, $P_r(0) = 1$, $P_c(0) = 1$.

Parameter	Values	
	$D.F.E\ (\mathscr{P}_1)$	$E.E.P(\mathscr{P}_2)$
r	2.1528	2.1528
k	100.0357	100.0357
β	0.123	0.623
α_1	0.4	0.044
α_2	0.6	0.6
β_1	0.0679	0.0679
γ	0.5	0.3333
μ	0.05	0.526
μ_1	0.01	0.1
ξ	0.003	0.003
σ	0.23	0.23
δ	0.04	0.04
γ_1	0.6	0.6

TABLE 2. Parameters and their corresponding values.

For the parametric values as mentioned in the 2^{nd} column of Table 2, the equilibrium point is $\mathscr{P}_1 = (100.0357, 0, 0, 0, 0)$, and the value of $R_0 = 0.5357 < 1$. The coefficients of characteristic equation (14) are $H_{11} = 3.2807,\ H_{12} = 2.80721,\ H_{13} = 0.86363,\ H_{14} = 0.104366,\ H_{15} = 0.00428943$, which are all positive. Thus, by using Lemma 7, the equilibrium point $\mathscr{P}_1$ is stable, which can also be verified from Figure 1a.

The equilibrium point obtained from the parameteric values as mentioned in the 3^{rd} column of Table 2 is $\mathscr{P}_2 = (56.4174, 55.2990, 27.6744, 1.0798, 0.8527)$, and the value of $R_0 = 12.0273 > 1$. The numerical values for coefficients of Equation (15) are $H_{21} = 5.07332,\ H_{22} = 8.76988,\ H_{23} = 6.91144,\ H_{24} = 2.5493,\ H_{25} = 0.355562$. These values satisfy condition (5) of Lemma 7, therefore establishing the stability of the equilibrium point $\mathscr{P}_2$, which is further solidified by Figure 1b.

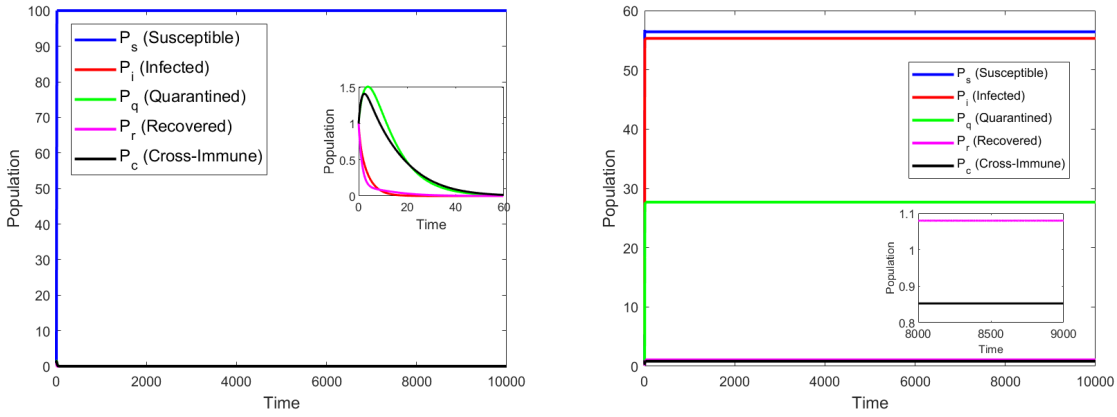

(A) *D.F.E* ($\mathscr{P}_1$) (B) *E.E.P* ($\mathscr{P}_2$)

FIGURE 1. Time-Series Plots of model (6).

Furthermore, to investigate the effect of the fractional order α on the dynamics of model (6), we conducted numerical simulations for different values of $\alpha = 0.9, 0.95, 1$. This allows us to analyze how varying α affects the stability and long-term behavior of model (6). The results are presented in Figure 2, which illustrates the behavior of the susceptible, infected, quarantined, recovered, and cross-immune sub-populations, respectively.

Figure 2a illustrates how the susceptible sub-population varies with time for different values of α ($\alpha = 0.9, 0.95, 1$). Notably, when $\alpha = 1$, the peak value of the solution curve is higher and it flattens quickly to attain the steady state. In contrast, as α decreases, the peak value diminishes, and the system takes longer to stabilize. A similar pattern is observed in Figures 2b and 2c, which depict the infected and quarantined sub-populations, respectively. In Figures 2d and 2e, the recovered and cross-immune sub-populations initially exhibit a dip, which is most pronounced for $\alpha = 1$, before rising to a peak, also maximized at $\alpha = 1$, and eventually settling into the steady state. Lower values of α result in a smaller initial dip, a lower peak, and a slower approach to the steady state.

The impact of certain model parameters (α_2, β_1, γ_1, σ) on the infected population P_i, for fractional order $\alpha = 0.9$, is illustrated in Figure 3. Figure 3a shows that as α_2 increases, P_i decreases, indicating that a higher inhibitory effect reduces the number of infectives. Figure 3b demonstrates that as β_1 increases, it results to a increase in the count of infected individuals, suggesting that a

faster transition of individuals from cross-immune to re-susceptible leads to heightened disease transmission. Similarly, in Figure 3c, a higher γ_1 results in greater number of infectives. This implies that, as recovered individuals lose total immunity and become cross-immune at a higher rate, the pool of individuals partially vulnerable to the disease increases resulting in more people getting infected. Figure 3d reveals that with a rise in σ, ${}^{C}D^{\alpha}P_i(t)$ also increases, highlighting that a higher reinfection probability, i. e., lower partial immunity of cross-immune individuals, results in a higher count of infectives.

However, when the inhibitory factor α_2 has a significantly low value, there is a drastic shift in the system's behavior, as observed in Figure 4, for which the parameteric values are chosen as in the 3^{rd} column of Table 2 except for α_2, which is set to $\alpha_2 = 0.0679$. Figure 4a depicts the dynamics of the susceptible sub-population over time for different values of $\alpha = 0.9, 0.95, 1$. For $\alpha = 1$, the system displays greater oscillatory behavior, whereas as α decreases, the oscillations diminish and the system reaches its steady state more quickly. Figures 4b, 4c, 4d and 4e show the influence of varying α on the infected, quarantined, recovered and cross-immune sub-populations, respectively, where similar trends of lower oscillations and faster attainment of steady state of the system are observed. Thus, the inhibitory factor α_2 is an important parameter that notably affect the system's behavior, leading to drastic changes as its value shifts from high to low. These simulation results underscore the substantial impact of the fractional order α on the dynamics of model (6), demonstrating the robustness of fractional differential equations in epidemiological modeling by enabling the selection of an optimal α to fit real-world data.

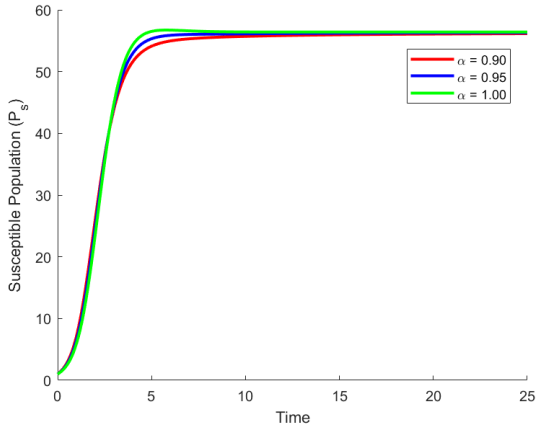

(A) P_s vs t ($\alpha = 0.9, 0.95, 1$)

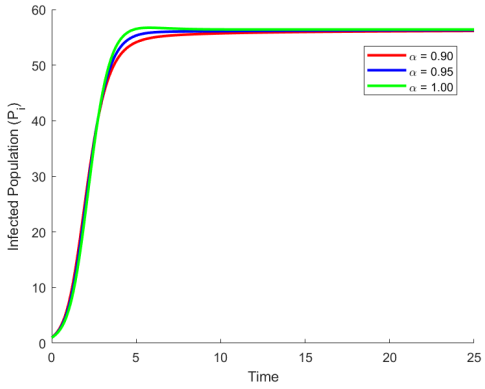

(B) P_i vs t ($\alpha = 0.9, 0.95, 1$)

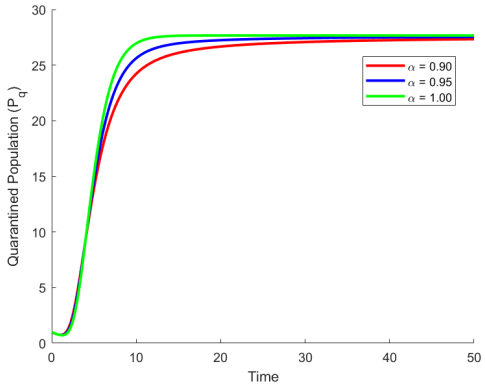

(C) P_q vs t ($\alpha = 0.9, 0.95, 1$)

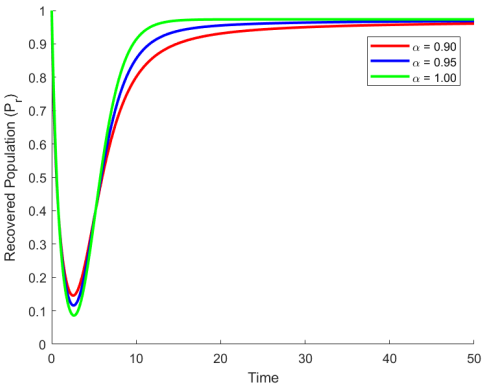

(D) P_r vs t ($\alpha = 0.9, 0.95, 1$)

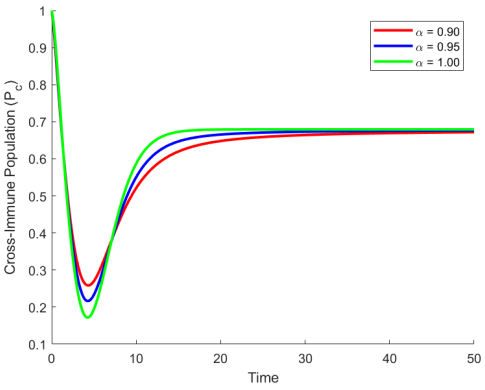

(E) P_c vs t ($\alpha = 0.9, 0.95, 1$)

FIGURE 2. Variation of the sub-populations with respect to time for varying fractional order α ($\alpha = 0.9, 0.95, 1$).

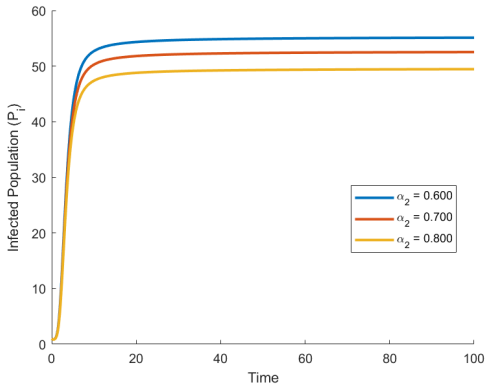

(A) P_i vs t for $\alpha_2 = 0.6, 0.7, 0.8$

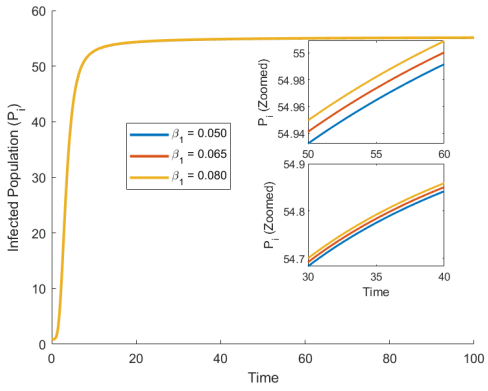

(B) P_i vs t for $\beta_1 = 0.05, 0.065, 0.08$

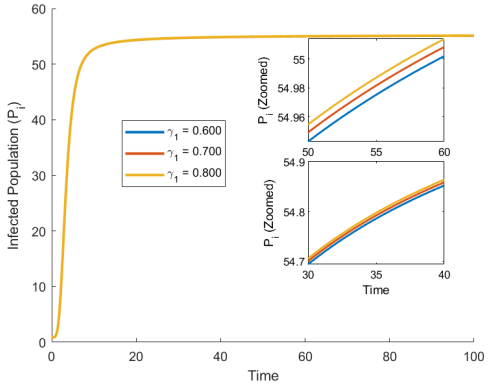

(C) P_i vs t for $\gamma_1 = 1.5, 1.888, 2.2$

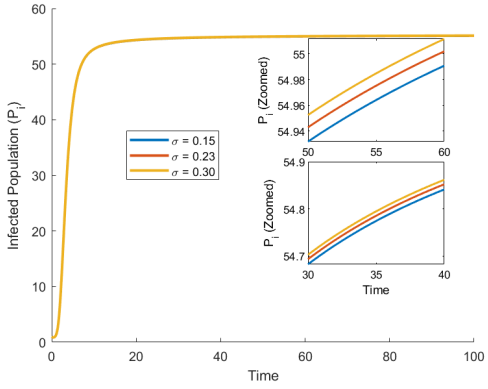

(D) P_i vs t for $\sigma = 0.15, 0.23, 0.3$

FIGURE 3. Variation of $P_i(t)$ with respect to time, at fractional order $\alpha = 0.9$, for different values of α_2, β_1, γ_1, σ.

5.1. Global Sensitivity Analysis of the Basic Reproduction Number. We employ Latin Hypercube Sampling (LHS) [29] to systematically assess the impact of each parameter on the basic reproduction number R_0 within defined uncertainty intervals. By computing Partial Rank Correlation Coefficients (PRCCs), we quantify the strength and direction of the relationship between R_0 and each parameter within it, as given by equation (13). The PRCC values, ranging from -1 to 1, indicate the degree of correlation, while their sign determines whether the effect is positive or negative. Higher absolute PRCC values signify stronger correlation. Assuming the parameters follow a uniform distribution, we calculate the PRCC values using 1000 simulations per run. This global sensitivity analysis of R_0 is illustrated in Figure 5.

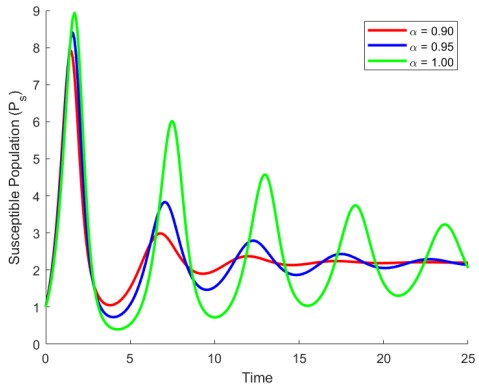

(A) P_s vs t ($\alpha = 0.9, 0.95, 1$)

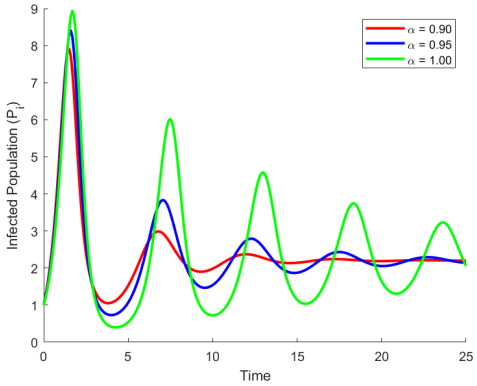

(B) P_i vs t ($\alpha = 0.9, 0.95, 1$)

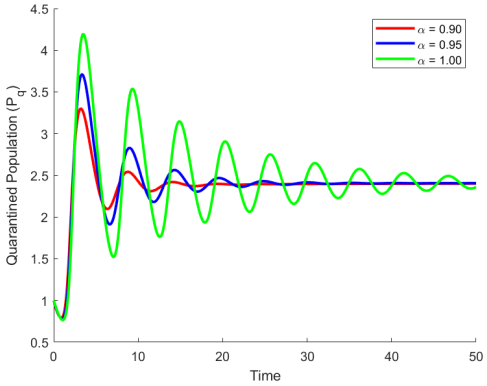

(C) P_q vs t ($\alpha = 0.9, 0.95, 1$)

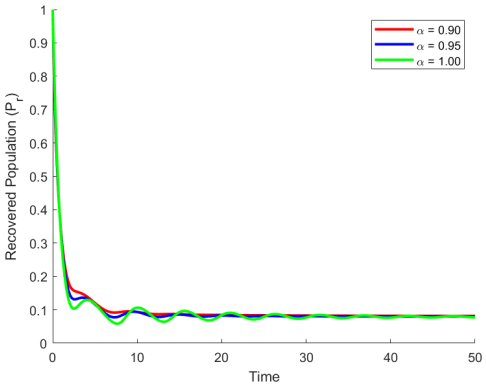

(D) P_r vs t ($\alpha = 0.9, 0.95, 1$)

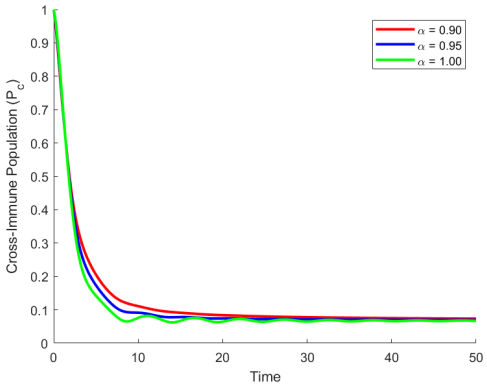

(E) P_c vs t ($\alpha = 0.9, 0.95, 1$)

FIGURE 4. Variation of the sub-populations with respect to time for varying fractional order α ($\alpha = 0.9, 0.95, 1$), for a lower value of α_2, ($\alpha_2 = 0.0679$).

From Figure 5, it is evident that the transmission rate β exhibits a strong positive correlation with R_0, indicating that an increase in β leads to a significant rise in R_0. The carrying capacity k of the susceptible population also shows a positive correlation, though slightly weaker, suggesting that a larger susceptible pool supports higher transmission potential. In contrast, the inhibitory factor α_1, the quarantine rate γ, the natural mortality rate μ and the disease-inducted death rate μ_1 all display negative correlations with R_0. Based on this global sensitivity analysis of R_0, adopting inhibitory measures such as social distancing, strengthening quarantine measures and reducing the disease transmission rate via public health interventions are key strategies for controlling disease spread.

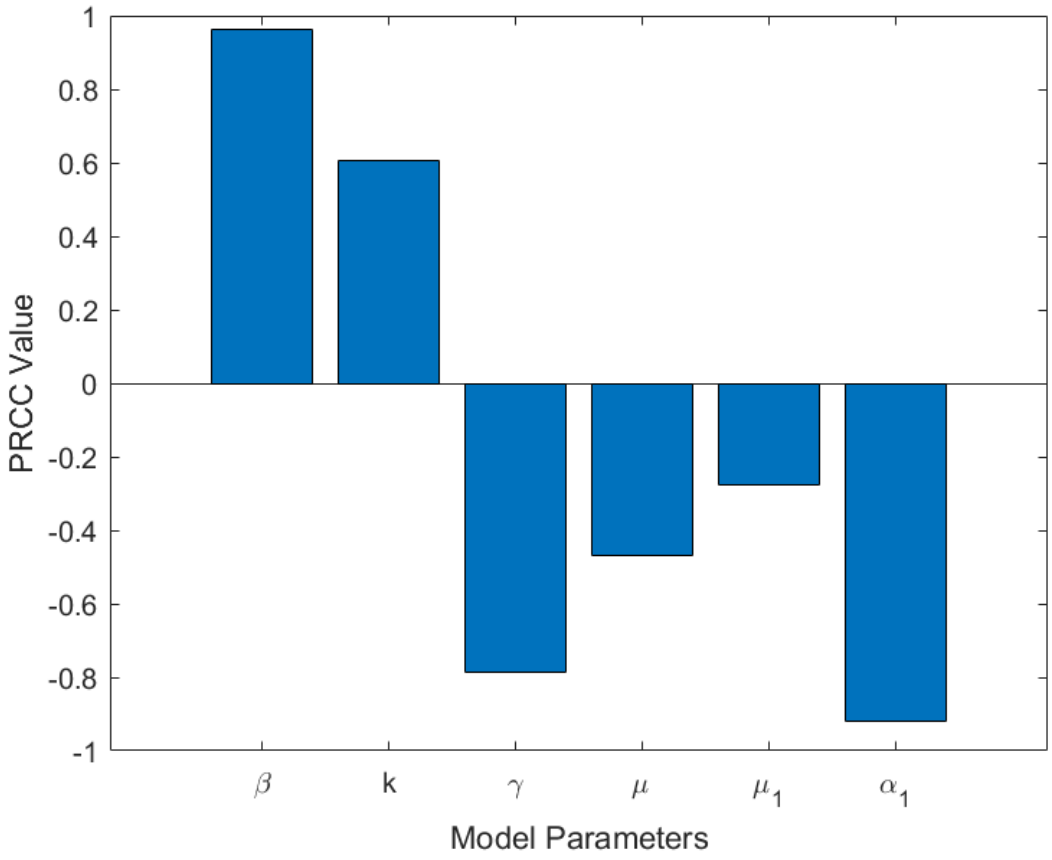

FIGURE 5. The Global Sensitivity Analysis of the Basic Reproduction Number R_0

6. CONCLUSION

This study focuses on developing and analyzing a fractional-order model (6). The mathematical analysis shows that the model maintains non-negative and bounded solutions, highlighting its biological relevance. Two key equilibria were identified: the $D.F.E$ ($\mathscr{P}_1$) and the $E.E.P$ ($\mathscr{P}_2$). The basic reproduction number is determined using the Next-Generation Matrix method, and it was shown that when R_0 is below one, then $\mathscr{P}_1$ remains locally asymptotically stable, but becomes unstable when R_0 surpasses one. Criteria's for local stability of $\mathscr{P}_2$ were obtained and stated in Theorem 2. Additionally, the global stability of the $E.E.P$ was examined, confirming that $\mathscr{P}_2$ achieves global stability under certain conditions on the parameters, using Lyapunov functions.

The numerical simulations aligned with the theoretical findings of this work. Figure 1a supports our analytical results that the $D.F.E$ ($\mathscr{P}_1$) remains locally asymptotically stable for $R_0 < 1$. The $E.E.P$ $\mathscr{P}_2$ is locally asymptotically stable, as it satisfies condition (5) of Lemma 7 for the parameter values used. This is further reinforced by the observations in Figure 1b. Figure 2 demonstrates the influence of the fractional order α on the dynamics of the system, showing that lower values of α lead to a smaller peak and slower approach to steady state across all sub-populations. Figure 3 illustrates how certain model parameters (α_2, β_1, γ_1, σ) affect the trajectory of $P_i(t)$ over time, for fractional order $\alpha = 0.9$, giving information about the impact of these parameters on the infected population. The variation in the dynamics of each of the sub-populations for different values of the fractional order α is also examined for a low value of the inhibitory factor α_2. Figure 4 indicates that a lower fractional order results in damped oscillations of the system, allowing it to attain its steady state faster. The global sensitivity analysis of the basic reproduction number R_0 was carried out to identify which parameters affect R_0 the most, offering valuable insights to policy makers on potential effective strategies to mitigate disease spread. This research underscores the critical role of fractional-order modeling in capturing the complex dynamics of disease transmission, providing deeper insights into system behavior and control strategies.

APPENDIX

$$
\begin{aligned}
F_1 &= (\beta\alpha_2\hat{e_2} - \alpha_1\alpha_2\hat{e_4})(\hat{e_2}^2 + \hat{e_4} + \hat{c_2} + \hat{a_7}\hat{e_2}\hat{e_4}^2),\\
F_2 &= (-\alpha_1\hat{e_4} + \beta\alpha_2\hat{e_1} - \alpha_1\alpha_2\hat{e_3} + \beta\hat{e_2})(\hat{e_2}^2 + \hat{e_4} + \hat{c_2} + \hat{a_7}\hat{e_2}\hat{e_4}^2)\\
&\quad +(\beta\alpha_2\hat{e_2} - \alpha_1\alpha_2\hat{e_4})(\hat{e_2}^2(\hat{e_3}\hat{c_2} + \hat{e_4}\hat{c_1}) + 2\hat{e_1}\hat{e_2}\hat{e_4}\hat{c_2} + \hat{a_6}\hat{e_2}^2\\
&\quad +\hat{a_7}\hat{e_1}\hat{e_4}^2 + 2\hat{e_3}\hat{e_4}\hat{a_7}\hat{e_2} + \hat{a_8}\hat{e_2}\hat{e_4}),\\
F_3 &= (\beta\hat{e_1} - \alpha_1\hat{e_3})(\hat{e_2}^2 + \hat{e_4} + \hat{c_2} + \hat{a_7}\hat{e_2}\hat{e_4}^2) + (-\alpha_1\hat{e_4} + \beta\alpha_2\hat{e_1} - \alpha_1\alpha_2\hat{e_3} + \beta\hat{e_2})\\
&\quad (\hat{e_2}^2(\hat{e_3}\hat{c_2} + \hat{e_4}\hat{c_1}) + 2\hat{e_1}\hat{e_2}\hat{e_4}\hat{c_2} + \hat{a_6}\hat{e_2}^2 + \hat{a_7}\hat{e_1}\hat{e_4}^2 + 2\hat{e_3}\hat{e_4}\hat{a_7}\hat{e_2} + \hat{a_8}\hat{e_2}\hat{e_4})\\
&\quad +(\beta\alpha_2\hat{e_2} - \alpha_1\alpha_2\hat{e_4})(\hat{e_2}^2\hat{e_4}\hat{c_2} + \hat{e_2}^2\hat{c_3}\hat{c_1} + 2\hat{e_1}\hat{e_2}(\hat{e_3}\hat{c_2} + \hat{e_4}\hat{c_1}) + 2\hat{e_1}\hat{e_2}\hat{a_6}\\
&\quad +2\hat{e_3}\hat{e_4}\hat{a_7}\hat{e_1} + \hat{a_7}\hat{e_2}\hat{e_3}^2 + \hat{a_8}\hat{e_1}\hat{e_4} + \hat{a_8}\hat{e_2}\hat{e_3}),\\
F_4 &= (\beta\hat{e_1} - \alpha_1\hat{e_3})(\hat{e_2}^2(\hat{e_3}\hat{c_2} + \hat{e_4}\hat{c_1}) + 2\hat{e_1}\hat{e_2}\hat{e_4}\hat{c_2} + \hat{a_6}\hat{e_2}^2 + \hat{a_7}\hat{e_1}\hat{e_4}^2 + 2\hat{e_3}\hat{e_4}\hat{a_7}\hat{e_2} + \hat{a_8}\hat{e_2}\hat{e_4})\\
&\quad +(-\alpha_1\hat{e_4} + \beta\alpha_2\hat{e_1} - \alpha_1\alpha_2\hat{e_3} + \beta\hat{e_2})(\hat{e_2}^2\hat{e_4}\hat{c_2} + \hat{e_2}^2\hat{c_3}\hat{c_1} + 2\hat{e_1}\hat{e_2}(\hat{e_3}\hat{c_2} + \hat{e_4}\hat{c_1})\\
&\quad +2\hat{e_1}\hat{e_2}\hat{a_6} + 2\hat{e_3}\hat{e_4}\hat{a_7}\hat{e_1} + \hat{a_7}\hat{e_2}\hat{e_3}^2 + \hat{a_8}\hat{e_1}\hat{e_4} + \hat{a_8}\hat{e_2}\hat{e_3})\\
&\quad +(\beta\alpha_2\hat{e_2} - \alpha_1\alpha_2\hat{e_4})(\hat{e_1}^2(\hat{e_3}\hat{c_2} + \hat{e_4}\hat{c_1}) + 2\hat{e_1}\hat{e_2}\hat{c_3}\hat{c_1} + \hat{e_1}^2\hat{a_6} + \hat{a_7}\hat{e_1}\hat{e_3}^2 + \hat{a_8}\hat{e_1}\hat{e_3}),\\
F_5 &= (\beta\hat{e_1} - \alpha_1\hat{e_3})(\hat{e_2}^2\hat{e_4}\hat{c_2} + \hat{e_2}^2\hat{c_3}\hat{c_1} + 2\hat{e_1}\hat{e_2}(\hat{e_3}\hat{c_2} + \hat{e_4}\hat{c_1}) + 2\hat{e_1}\hat{e_2}\hat{a_6} + 2\hat{e_3}\hat{e_4}\hat{a_7}\hat{e_1}\\
&\quad +\hat{a_7}\hat{e_2}\hat{e_3}^2 + \hat{a_8}\hat{e_1}\hat{e_4} + \hat{a_8}\hat{e_2}\hat{e_3}) + (-\alpha_1\hat{e_4} + \beta\alpha_2\hat{e_1} - \alpha_1\alpha_2\hat{e_3} + \beta\hat{e_2})(\hat{e_1}^2(\hat{e_3}\hat{c_2} + \hat{e_4}\hat{c_1})\\
&\quad +2\hat{e_1}\hat{e_2}\hat{c_3}\hat{c_1} + \hat{e_1}^2\hat{a_6} + \hat{a_7}\hat{e_1}\hat{e_3}^2 + \hat{a_8}\hat{e_1}\hat{e_3}) + (\beta\alpha_2\hat{e_2} - \alpha_1\alpha_2\hat{e_4})(\hat{e_1}^2\hat{e_3}\hat{c_1}),\\
F_6 &= (\beta\hat{e_1} - \alpha_1\hat{e_3})(\hat{e_1}^2(\hat{e_3}\hat{c_2} + \hat{e_4}\hat{c_1}) + 2\hat{e_1}\hat{e_2}\hat{c_3}\hat{c_1} + \hat{e_1}^2\hat{a_6} + \hat{a_7}\hat{e_1}\hat{e_3}^2 + \hat{a_8}\hat{e_1}\hat{e_3})\\
&\quad +(-\alpha_1\hat{e_4} + \beta\alpha_2\hat{e_1} - \alpha_1\alpha_2\hat{e_3} + \beta\hat{e_2})(\hat{e_1}^2\hat{e_3}\hat{c_1}),\\
F_7 &= (\beta\hat{e_1} - \alpha_1\hat{e_3})(\hat{e_1}^2\hat{e_3}\hat{c_1}).
\end{aligned}
$$

Here,

$$
\begin{aligned}
\hat{e_1} &= (\mu+\gamma_1)(\mu+\delta+\mu_1)(\mu+\beta_1),\\
\hat{e_2} &= \xi(\mu+\gamma_1)(\mu+\delta+\mu_1) - (1-\sigma)\gamma_1\xi,\\
\hat{e_3} &= (\mu+\gamma_1)(\mu+\delta+\mu_1)(\mu+\beta_1)(\mu+\gamma+\mu_1),\\
\hat{e_4} &= (\mu+\gamma_1)(\mu+\delta+\mu_1)(\mu+\gamma+\mu_1)\xi - (1-\sigma)\gamma_1\xi - \sigma\xi\delta\gamma\gamma_1,\\
\hat{c_1} &= \beta\hat{e_1},\\
\hat{c_2} &= \alpha_1,\\
\hat{c_3} &= \beta\alpha_2,\\
\hat{c_4} &= \alpha_1\alpha_2,\\
\hat{a_1} &= \beta rk,
\end{aligned}
$$

$$\begin{aligned}
\hat{a_2} &= \beta, \\
\hat{a_3} &= \beta\alpha_2 rk, \\
\hat{a_4} &= \beta, \\
\hat{a_5} &= \beta^2 k, \\
\hat{a_6} &= \beta^2\beta_1 k\delta\gamma\gamma_1, \\
\hat{a_7} &= \beta k\alpha_1, \\
\hat{a_8} &= \beta\beta_1\delta\gamma\gamma_1\alpha_1 k.
\end{aligned}$$

CONFLICT OF INTERESTS

The authors declare that there is no conflict of interests.

REFERENCES

[1] WHO, WHO COVID-19 Dashboard. https://data.who.int/dashboards/covid19/cases?n=c.

[2] WHO, the Burden of Influenza. https://www.who.int/news-room/feature-stories/detail/the-burden-of-influenza.

[3] W.O. Kermack, A.G. McKendrick, A Contribution to the Mathematical Theory of Epidemics, Proc. R. Soc. Lond. Ser. A 115 (1927), 700–721. https://doi.org/10.1098/rspa.1927.0118.

[4] E. Avila-Vales, Á.G. Pérez, Dynamics of a Time-Delayed Sir Epidemic Model with Logistic Growth and Saturated Treatment, Chaos Solitons Fractals 127 (2019), 55–69. https://doi.org/10.1016/j.chaos.2019.06.024.

[5] D.J. Gerberry, F.A. Milner, An Seiqr Model for Childhood Diseases, J. Math. Biol. 59 (2008), 535–561. https://doi.org/10.1007/s00285-008-0239-2.

[6] C. Castillo-Chavez, Z. Feng, Mathematical Models for the Disease Dynamics of Tuberculosis, in: Fourth International Conference on Mathematical Population Dynamics, 1995.

[7] D. Wodarz, M.A. Nowak, Mathematical Models of Hiv Pathogenesis and Treatment, BioEssays 24 (2002), 1178–1187. https://doi.org/10.1002/bies.10196.

[8] S. Edward, A Mathematical Model for Control and Elimination of the Transmission Dynamics of Measles, Appl. Comput. Math. 4 (2015), 396–408.. https://doi.org/10.11648/j.acm.20150406.12.

[9] R. Casagrandi, L. Bolzoni, S.A. Levin, V. Andreasen, The SIRC Model and Influenza A, Math. Biosci. 200 (2006), 152–169. https://doi.org/10.1016/j.mbs.2005.12.029.

[10] S. Goel, S.K. Bhatia, J.P. Tripathi, et al. SIRC Epidemic Model with Cross-Immunity and Multiple Time Delays, J. Math. Biol. 87 (2023), 42. https://doi.org/10.1007/s00285-023-01974-w.

[11] H. Youssef, N. Alghamdi, M.A. Ezzat, A.A. El-Bary, A.M. Shawky, Study on the Seiqr Model and Applying the Epidemiological Rates of Covid-19 Epidemic Spread in Saudi Arabia, Infect. Dis. Model. 6 (2021), 678–692. https://doi.org/10.1016/j.idm.2021.04.005.

[12] H.P. Singh, S.K. Bhatia, Y. Bahri, R. Jain, Optimal Control Strategies to Combat Covid-19 Transmission: a Mathematical Model with Incubation Time Delay, Results Control. Optim. 9 (2022), 100176. https://doi.org/10.1016/j.rico.2022.100176.

[13] F. Rihan, C. Rajivganthi, Dynamics of Fractional-Order Delay Differential Model of Prey-Predator System with Holling-Type Iii and Infection Among Predators, Chaos, Solitons Fractals 141 (2020), 110365. https://doi.org/10.1016/j.chaos.2020.110365.

[14] A.A.M. Arafa, S.Z. Rida, M. Khalil, A Fractional-Order Model of Hiv Infection: Numerical Solution and Comparisons with Data of Patients, Int. J. Biomath. 07 (2014), 1450036. https://doi.org/10.1142/s1793524514500363.

[15] R.T. Alqahtani, Mathematical Model of Sir Epidemic System (covid-19) with Fractional Derivative: Stability and Numerical Analysis, Adv. Differ. Equ. 2021 (2021), 2. https://doi.org/10.1186/s13662-020-03192-w.

[16] M.B. Ghori, P.A. Naik, J. Zu, Z. Eskandari, M. Naik, Global Dynamics and Bifurcation Analysis of a Fractional-order Seir Epidemic Model with Saturation Incidence Rate, Math. Methods Appl. Sci. 45 (2022), 3665–3688. https://doi.org/10.1002/mma.8010.

[17] A.K. Rajak, Nilam, A Fractional-Order Epidemic Model with Quarantine Class and Nonmonotonic Incidence: Modeling and Simulations, Iran. J. Sci. Technol. Trans. A: Sci. 46 (2022), 1249–1263. https://doi.org/10.1007/s40995-022-01339-w.

[18] S. Paul, A. Mahata, S. Mukherjee, B. Roy, Dynamics of Siqr Epidemic Model with Fractional Order Derivative, Partial. Differ. Equ. Appl. Math. 5 (2022), 100216. https://doi.org/10.1016/j.padiff.2021.100216.

[19] S. Askar, D. Ghosh, P. Santra, A.A. Elsadany, G. Mahapatra, A Fractional Order Sitr Mathematical Model for Forecasting of Transmission of Covid-19 of India with Lockdown Effect, Results Phys. 24 (2021), 104067. https://doi.org/10.1016/j.rinp.2021.104067.

[20] H. Li, S. Guo, Dynamics of a SIRC Epidemiological Model, Electron. J. Differ. Equ. 2017 (2017), 121.

[21] Z.M. Odibat, N.T. Shawagfeh, Generalized Taylor's Formula, Appl. Math. Comput. 186 (2007), 286–293. https://doi.org/10.1016/j.amc.2006.07.102.

[22] A. Boukhouima, K. Hattaf, N. Yousfi, Dynamics of a Fractional Order Hiv Infection Model with Specific Functional Response and Cure Rate, Int. J. Differ. Equ. 2017 (2017), 1–8. https://doi.org/10.1155/2017/8372140.

[23] E. Ahmed, A. El-Sayed, H. El-Saka, Equilibrium Points, Stability and Numerical Solutions of Fractional-Order Predator–prey and Rabies Models, J. Math. Anal. Appl. 325 (2007), 542–553. https://doi.org/10.1016/j.jmaa.2006.01.087.

[24] A. Kumar, Stability of a Fractional-Order Epidemic Model with Nonlinear Incidences and Treatment Rates, Iran. J. Sci. Technol. Trans. A: Sci. 44 (2020), 1505–1517. https://doi.org/10.1007/s40995-020-00960-x.

[25] Z. Lu, Y. Zhu, Comparison Principles for Fractional Differential Equations with the Caputo Derivatives, Adv. Differ. Equ. 2018 (2018), 237. https://doi.org/10.1186/s13662-018-1691-y.

[26] P. Van Den Driessche, J. Watmough, Further Notes on the Basic Reproduction Number, in: F. Brauer, P. Van Den Driessche, J. Wu (Eds.), Mathematical Epidemiology, Springer, Berlin, 2008: pp. 159–178. https://doi.org/10.1007/978-3-540-78911-6_6.

[27] D. Matignon, Stability Results for Fractional Differential Equations With Applications to Control Processing, in: Computational Engineering in Systems Applications, Vol. 2, pp. 963–968, (1996).

[28] J.P. LaSalle, The Stability of Dynamical Systems, SIAM, (1976).

[29] S. Marino, I.B. Hogue, C.J. Ray, D.E. Kirschner, A Methodology for Performing Global Uncertainty and Sensitivity Analysis in Systems Biology, J. Theor. Biol. 254 (2008), 178–196. https://doi.org/10.1016/j.jtbi.2008.04.011.